Improving Land Cover Mapping in Riverine Environments with Machine Learning and Spectral Indices

Rohit Sharma[1], Pritipadmaja[1], Zulfequar Ahmad[1], Rahul Dev Garg[1]

[1]Department of Civil Engineering, Indian Institute of Technology Roorkee, Roorkee, India – r_sharma@ce.iitr.ac.in

Keywords: LISS-4 imagery, Random Forest, Support Vector Machine, Gradient Tree Boosting, Water channel delineation.

Abstract

Accurate land cover classification in riverine environments is essential for understanding hydrological dynamics, ecological health, and resource management. This study utilizes high-resolution LISS-4 imagery from the IRS-R2 satellite to address the complex classification challenges in the dynamic confluence of the Mahanadi and Shivnath Rivers. To enhance classification accuracy, two distinct feature sets were developed: the first feature set (FS-1) contained the original three spectral bands of the imagery, and the second feature set (FS-2) added eight derived spectral indices to improve class separation. Three machine learning classifiers, Random Forest (RF), Support Vector Machine (SVM), and Gradient Tree Boosting (GTB), were applied to assess the effectiveness of each feature set. The results demonstrated that the combination of FS-2 and RF yielded the most accurate and interpretable classification, achieving an overall accuracy of 84.48% and a Cohen's Kappa coefficient of 0.81. Visual results demonstrated precise delineation of narrow water channels and sandbars, when using the enhanced feature set FS-2 with the Random Forest (RF) classifier, the model achieved an F1-score of 86.96% for dense vegetation and 83.78% for water. FS-2 consistently improved F1-scores across all classifiers, aiding in distinguishing visually similar classes like wet sand, dry sand, and sparse vegetation. These findings highlight the value of combining spectral indices with high-resolution imagery to achieve accurate land cover classification in complex landscapes, supporting applications in ecological monitoring, flood risk assessment, and resource management for riverine ecosystems.

1. Introduction

Classifying land cover from satellite imagery is fundamental for understanding and managing diverse ecosystems (Foody, 2002). In riverine environment, where shifting patterns of water, vegetation, and sediment create complex landscapes, precise classification is especially important for effective flood management, habitat protection, and resource planning (Boothroyd et al., 2021). With the increasing availability of high-resolution remote sensing data, advancements in machine learning (ML) algorithms have been pivotal in enhancing classification accuracy across varied land cover types. Several studies underscore the effectiveness of algorithms like Random Forest (RF), Support Vector Machine (SVM), and Convolutional Neural Networks (CNNs) when used with satellite imagery data (Rahman et al., 2020; Talukdar et al., 2020; Ouchra et al., 2023). These classifiers benefit substantially from the integration of spectral indices, which amplify specific land cover characteristics such as vegetation health and water content, thereby improving the accuracy of classification outputs (Verma et al., 2016; Arora et al., 2020; Tadese et al., 2020).

Riverine landscapes, characterized by narrow water bodies, diverse vegetation types, and sedimentary features, present unique classification challenges due to the similarity of spectral signatures between classes like wet sand, dry sand, and sparse vegetation. Studies demonstrate that spectral indices such as the Normalized Difference Vegetation Index (NDVI) and Normalized Difference Water Index (NDWI) enhance feature separability in these environments, contributing to accurate mapping of land cover (Boothroyd et al., 2021; Tobón-Marín and Barriga, 2020). Furthermore, texture-based features derived from high-resolution imagery capture spatial patterns at finer scales, which improves the detection of landscape structures in heterogeneous areas (Vishnoi and Pareek, 2024; Arora et al., 2020).

The application of advanced machine learning classifiers has gained traction in recent years due to their adaptability to high-dimensional and complex data. RF, for example, is noted for its robustness and stability, especially in diverse landscape classification, while SVM has proven effective in high-dimensional feature spaces, such as when spectral and textural indices are combined (Boothroyd et al., 2021; Tobón-Marín and Barriga, 2020). CNNs, meanwhile, have demonstrated high accuracy in LISS-IV image classification when combined with object-based deep feature extraction, which significantly improves classification precision by preserving edge details (Rajesh et al., 2019; Vishnoi and Pareek, 2024). Moreover, feature selection techniques such as correlation-based feature selection (CFS) have been shown to reduce data redundancy and computational costs, thus optimizing the classifier's efficiency and accuracy (Zhang et al., 2023; Arora et al., 2020).

Recent research emphasizes the role of cloud-based platforms, like Google Earth Engine (GEE), in facilitating large-scale spatial analyses. These platforms overcome storage and processing limitations, allowing for multitemporal analysis of river morphology and land cover dynamics across wide spatial scales. By enabling the integration of diverse datasets, including Landsat and Sentinel imagery, GEE has proven invaluable for the study of geomorphic features, particularly in assessing temporal changes in riverine environments (Tobón-Marín and Barriga, 2020; Boothroyd et al., 2021).

In this study, we employ a feature-rich approach integrating spectral bands and indices from high-resolution LISS-IV imagery with machine learning classifiers, RF, SVM, and Gradient Tree Boosting (GTB) for evaluating classification

https://doi.org/10.5194/isprs-annals-X-G-2025-813-2025

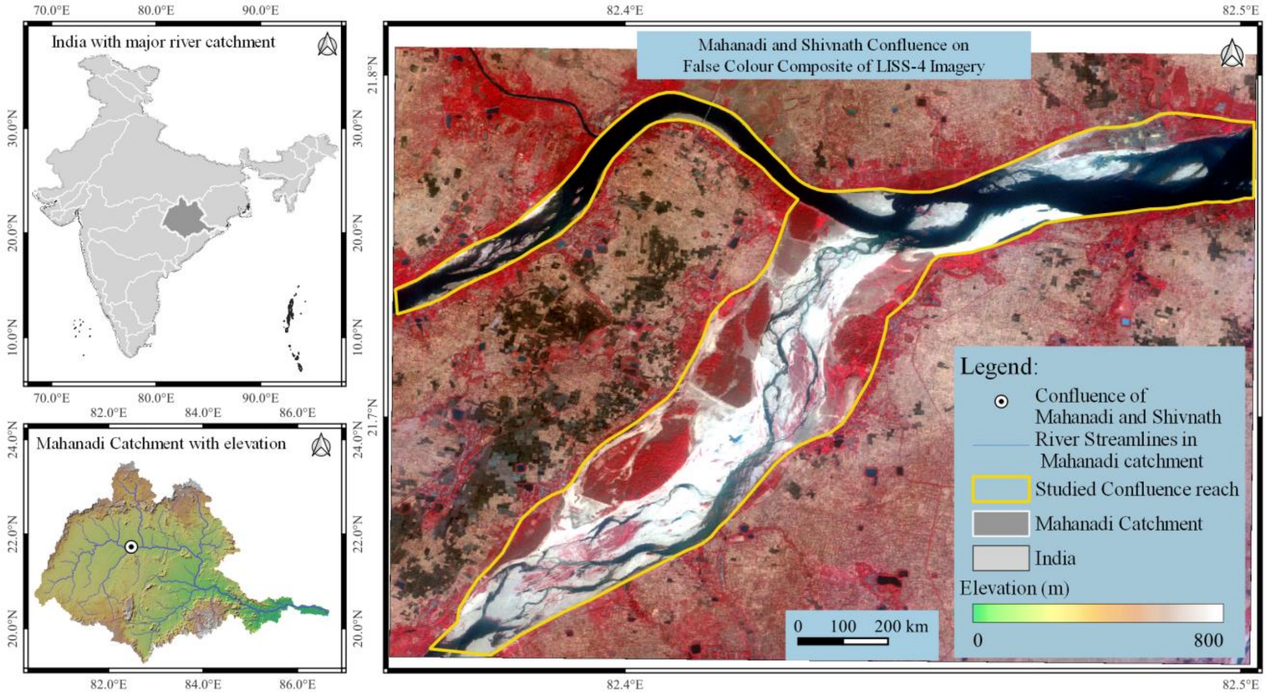

Figure 1. Study area map

performance in the dynamic confluence of the Mahanadi and Shivnath Rivers in Chhattisgarh state of India (Figure 1). This region was chosen for its dynamic and diverse land cover, which includes water bodies, wet and dry sand deposits, sparse vegetation, and dense vegetation, making it an ideal environment for testing riverine land cover classification. By capturing the natural variability across these complex landscape features, our approach aims to address the limitations of previous methodologies, enhancing classification accuracy and offering actionable insights for riverine ecosystem management, sustainable resource planning, and environmental conservation.

2. Data and Methods

2.1 Dataset

For this study, we utilized Linear Imaging Self-Scanning Sensor 4 (LISS-4) satellite imagery provided by the National Remote Sensing Centre (NRSC), India. The image was acquired on January 1, 2024, from the Indian Remote Sensing Satellite (IRS-R2). This high-resolution imagery has a nominal spatial resolution of 5.8 meters, with three spectral bands: Green, Red, and Near-Infrared (NIR). To ensure that the analysis focused solely on the riverine landscape, the banks of the river were manually digitized, and all subsequent processing was confined to the area within the river boundaries.

2.2 Feature set creation

A feature set represents the input data used for classification, and a robust feature set is essential for capturing the underlying characteristics of a landscape, especially in complex environments like riverine systems. To enhance model performance and ensure accurate classification, this study developed two distinct feature sets, combining spectral data and derived indices. These feature sets provide both reflectance information and biophysical insights, improving the model’s ability to differentiate between diverse land cover types.

The first feature set (FS-1) consisted of the three spectral bands from LISS-4: Green, Red, and Near-Infrared (NIR). These bands provide essential reflectance data, but they may not be sufficient to capture subtle differences in mixed land cover, such as distinguishing between wet and dry sand or sparse and dense vegetation. Therefore, additional indices were introduced in the second feature set to enrich the dataset.

The second feature set (FS-2) included the original three bands along with seven indices. These indices were selected to provide insights into vegetation health, water presence, and soil moisture, which are the key elements in riverine landscapes. The indices used in this study include the NDVI (Rouse et al., 1974), NDWI (McFeeters, 1996), Green-Red Vegetation Index (GRVI) (Gitelson et al., 1996), Soil Adjusted Vegetation Index (SAVI) (Huete, 1988), Optimised Soil Adjusted Vegetation Index (OSAVI) (Rondeaux et al., 1996), Water Index (WI) (Peñuelas et al., 1993) and Global Environment Monitoring Index (GEMI) (Pinty & Verstraete, 1992). The formulas and descriptions for these indices are provided in Table 1. Together, these indices provide detailed insights into vegetation, water bodies, and soil conditions, improving the reliability of land cover classification across the study area.

Combining raw spectral bands with indices helps enrich the dataset with more meaningful features that directly correlate with biophysical properties. Using both spectral bands and derived indices allows the classification models to address the heterogeneity and complexity of the riverine environment.

2.3 Land cover classes

The study focuses on classifying five key land cover classes within the riverine environment: water, dry sand, wet sand, sparse vegetation, and dense vegetation. These classes represent the dynamic elements of the confluence area of the Mahanadi and Shivnath Rivers, providing essential insights into the ecological and hydrological variability of the landscape.

https://doi.org/10.5194/isprs-annals-X-G-2025-813-2025

Index	Formula	Purpose	Characteristics
NDVI	(NIR - Red) / (NIR + Red)	Assesses vegetation health, vigor, and density	Values range from -1 to 1; higher values indicate denser vegetation, while lower values represent non-vegetated surfaces
NDWI	(Green - NIR) / (Green + NIR)	Enhances detection of open water bodies	Values range from -1 to 1; higher values indicate water presence, useful for mapping rivers and channels
GRVI	(Green – Red) / (Green + Red)	Distinguishes areas with active vegetation	Values range from -1 to 1; higher values indicate vegetation presence, aiding in vegetation pattern detection in riverine landscapes.
SAVI	((NIR – Red) * (1 + L) / (NIR + Red + L) where L = 0.5	Reduces soil brightness impact in sparse vegetation areas	Values range from -1 to 1; L is typically 0.5, effective for semi-arid areas with sparse vegetation
OSAVI	(NIR – Red) / (NIR + Red + 0.16)	Further reduces soil influence for sparse vegetation regions	Values range from -1 to 1; optimized for mixed soil and vegetation cover in floodplains
WI	NIR/Green	Measures water content on the surface	Lower values indicate wetter surfaces; useful for detecting moisture along riverbanks, floodplains, and wetlands.
GEMI	η = (2 *(NIR -Red) + 1.5*NIR + 0.5*Red) / (NIR + Red + 0.5), GEMI = (η* (1 – 0.25 * η) – ((Red – 0.125)/ (1 – Red))	Monitors vegetation under varying atmospheric conditions	GEMI reduces atmospheric effects and enhances vegetation detection, suitable for riverine and floodplain environments with fluctuating atmospheric conditions.

Table 1. Description of spectral indices

2.3.1 Water: Water bodies are a critical component of riverine systems, encompassing flowing rivers, stagnant pools, and small channels. In remote sensing, water is typically identified by its strong absorption of NIR radiation and higher reflectance in the Green band (McFeeters, 1996). Accurately mapping water bodies is essential for monitoring seasonal changes, flood events, and resource availability.

2.3.2 Dry Sand: Dry sand deposits are common along riverbanks, floodplains, and sandbars, especially during the dry season when river levels recede. These areas exhibit high reflectance across the visible spectrum and are often challenging to distinguish from other bright surfaces. Proper classification of dry sand helps in understanding sediment transport, erosion processes, and sand mining impacts.

2.3.3 Wet Sand: Wet sand refers to sand deposits that retain moisture from recent river flows or are submerged under shallow water. These areas are critical indicators of seasonal water dynamics and flooding patterns. Wet sand exhibits intermediate reflectance between dry sand and water, making its classification challenging without texture-based analysis.

2.3.4 Sparse Vegetation: Sparse vegetation covers areas with minimal plant density, including grasslands, shrublands, or degraded vegetation patches along the riverbanks. These areas play an essential role in preventing soil erosion and maintaining riverbank stability. Sparse vegetation is often characterized by low to moderate NDVI values, as it reflects more of the Red spectrum compared to dense vegetation (Huete, 1988).

2.3.5 Dense Vegetation: Dense vegetation refers to areas with high plant density, such as forests or thick riparian zones along the riverbanks. These regions exhibit high NDVI and NIR reflectance due to the abundance of chlorophyll. Mapping dense vegetation is important for understanding biodiversity, carbon sequestration, and the ecological health of the riverine landscape (Rouse et al., 1974).

This classification framework is designed to capture the essential features of the riverine system by effectively distinguishing between the spectral and textural characteristics of each land cover class. By addressing the unique spectral signatures and biophysical properties of water, dry sand, wet sand, sparse vegetation, and dense vegetation, this approach provides a comprehensive understanding of the ecological and hydrological dynamics at the confluence of the Mahanadi and Shivnath Rivers. This refined mapping enhances the accuracy of land cover classification and also supports informed resource management, conservation planning, and environmental monitoring in this sensitive riverine landscape.

2.4 Classification Algorithm

This study employed three widely used supervised machine learning classifiers: Random Forest (RF), Support Vector Machine (SVM), and Gradient Tree Boosting (GTB). These algorithms were chosen for their robustness, performance in remote sensing applications, and ability to handle both spectral and textural data (Belgiu & Drăguţ, 2016; Pal & Mather, 2005). Each classifier was trained using 30 points per class (a total of 150 points) to ensure a balanced representation of all five land cover types.

2.4.1 Random Forest (RF): RF is an ensemble learning algorithm that builds multiple decision trees and combines their predictions to improve accuracy (Breiman, 2001). Each tree is trained on a randomly selected subset of the data, reducing the risk of overfitting. RF can efficiently handle large datasets with high-dimensional features, such as those in remote sensing applications. Its robustness against noise and flexibility in dealing with both categorical and continuous data make it a popular choice for land cover classification.

2.4.2 Support Vector Machine (SVM): SVM is a powerful algorithm known for its ability to find the optimal hyperplane that maximally separates different classes (Cortes & Vapnik, 1995). It is particularly effective in high-dimensional spaces, making it suitable for remote sensing datasets with multiple features (Pal & Mather, 2005). SVM works well for complex classification tasks, even with a limited number of training samples, which is a common scenario in remote sensing studies.

2.4.3 Gradient Tree Boosting (GTB): GTB is a boosting algorithm that builds models sequentially, improving the prediction accuracy by minimizing errors made by previous models. This algorithm is highly effective for structured data and performs well in classification tasks with complex patterns (Natekin & Knoll, 2013). In remote sensing, GTB has been successfully used for land cover mapping due to its ability to handle both non-linear relationships and high-dimensional data (Rodriguez-Galiano et al., 2015).

All three classifiers, RF, SVM, and GTB, were applied to both the feature sets, resulting in a total of six classified images. This dual approach enabled a comprehensive evaluation of how well each feature set and classifier performed in mapping the riverine land cover types. The outcomes of these models were then assessed through accuracy metrics to determine the most effective combinations for the study area.

2.5 Accuracy Assessment

The accuracy assessment involved a total of 174 points carefully selected across the five land cover classes: 42 points for water, 30 for dense vegetation, 36 for wet sand, 26 for dry sand, and 40 for sparse vegetation. These points were chosen from challenging locations within the study area, where classifiers were expected to encounter difficulties due to spectral similarities and mixed boundaries. This included areas such as the transition zones between wet and dry sand, along water channels, narrow river sections, and the edges of sandbars. This strategic sampling allowed for a more rigorous test of the ability of the classifier to handle complex land cover scenarios, beyond simple homogeneous areas.

Following this sampling, the accuracy of the classification outputs was assessed using key metrics, including the confusion matrix, overall accuracy, Cohen's Kappa coefficient, and F1-Score by class. Each classified image was carefully evaluated to determine how well the classifiers distinguished between the five land cover classes, providing deeper insights into their strengths and limitations in mapping the complex riverine landscape.

The confusion matrix is a tabular representation that compares the predicted classifications with the actual ground truth data, providing insight into where misclassifications occur. Each row of the matrix represents the true class, and each column represents the predicted class, enabling a detailed analysis of which classes are confused with one another.

Overall accuracy measures the proportion of correctly classified points out of the total sampled points, offering a simple, yet broad indicator of the classifier's performance. It is calculated using the following formula:

$$\text{Overall Accuracy} = 100*(\text{Number of correctly Classified Points}/\ \text{Total Number of Points})$$

While it provides a useful summary, it does not account for chance agreement, which can sometimes inflate accuracy metrics, particularly when imbalanced class distributions. To address this limitation, the Cohen's Kappa coefficient (κ) is employed. Kappa adjusts for the likelihood of agreement occurring by chance, offering a more nuanced assessment of the classifier's reliability. The formula for Kappa is:

$$\kappa = (\rho_o - \rho_e) / (1 - \rho_e)$$

where ρ_o= observed agreement (the proportion of correctly classified points)
ρ_e= expected agreement by chance

A Kappa value close to 1 indicates strong agreement between the predicted and actual true classes, while values near 0 suggest the performance is no better than random chance.

Finally, the F1-Score balances two critical metrics: precision and recall. Precision measures the proportion of correctly predicted positive instances out of all predicted positives. In contrast, recall measures the proportion of correctly predicted positives out of all actual positives in the ground truth. The formula for the F1-Score is:

$$F1 = 2^* (\text{Precision} * \text{Recall}) / (\text{Precision} + \text{Recall})$$

where Precision = (TP) / (TP + FP), and
Recall = (TP) / (TP + FN)
TP is True Positive; FP is False Positive and FN is False Negative.

Together, these metrics provide a comprehensive evaluation framework for classification performance, highlighting both overall effectiveness and specific areas where classifiers may encounter challenges, such as distinguishing between closely related classes. While overall accuracy gives a general measure of success, Kappa accounts for chance agreement, and the F1-score offers class-level insights, which are particularly valuable for handling complex boundary regions and mixed land cover types.

In the following section, we apply these metrics to assess the performance of each classifier and feature set, establishing a robust basis for comparing their effectiveness in this complex riverine environment.

3. Results and Discussion

The classification results were obtained by applying three machine learning algorithms, RF, SVM, and GTB, on two distinct feature sets (FS-1 and FS-2) and are presented in Figure 2 along with their respective confusion matrices. The classified images were carefully interpreted to analyze the spatial distribution of the identified land cover types, providing insights into the landscape's composition and variability. The interpretation focused on assessing how well the classifiers handled the spectral and spatial variability within the riverine environment, highlighting the strengths and limitations of each feature set in capturing key land cover characteristics.

The inclusion of eight indices in FS-2 improved the classification performance across all classifiers, resulting in smoother, more coherent outputs with fewer instances of salt-and-pepper noise. RF and GTB both showed noticeable improvements in sandbar delineation when using FS-2, reducing misclassification of sand as sparse vegetation that was evident in FS-1. Specifically, in the RF classification for FS-2 classification, narrow water channels are well captured, demonstrating the importance of spectral indices in identifying subtle features within the riverine landscape. However, the same classifier struggled with separating wet sand from sparse vegetation, a challenge reflected in both the visual output and

https://doi.org/10.5194/isprs-annals-X-G-2025-813-2025 |

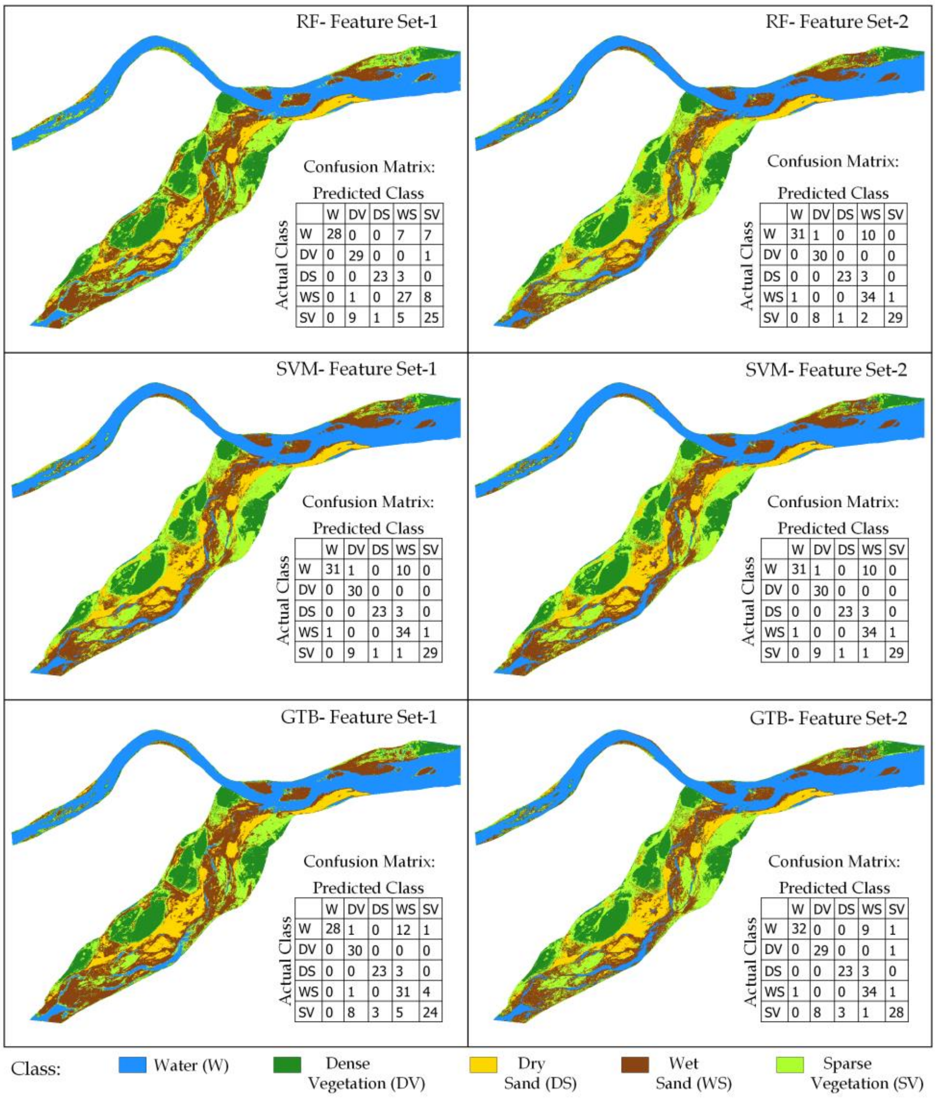

Figure 2. Land cover Classification and corresponding confusion matrices

the confusion matrix, where wet sand pixels were occasionally assigned as sparse vegetation.

While SVM showed relatively similar performance across FS-1 and FS-2, the smoothness of the output was slightly enhanced with FS-2. However, due to the absence of a built-up class in this study, hydraulic structures near the river, which should ideally be classified as sand due to their similar reflectance properties, were often misclassified as water because of their proximity to water bodies. This highlights the sensitivity of the SVM classifier to neighbouring spatial relationships. In contrast, RF and GTB tended to misclassify these structures as sparse vegetation and wet sand, respectively. Additionally, SVM encountered challenges in accurately mapping narrow water channels, where portions of these channels were incorrectly assigned as wet sand, as shown in the confusion matrices for both FS-1 and FS-2.

Among the classifiers, GTB produced relatively balanced outputs, but its performance was somewhat inconsistent with narrow water channels, particularly in FS-1. In these cases, GTB often misclassified wet sand as sparse vegetation or vice versa. However, when applied to FS-2, GTB demonstrated better separation of land cover types along sandbar edges, although it still underperformed slightly in identifying narrow water channels compared to RF. The confusion matrix for GTB of FS-2 reflects this, with more accurate identification of water and dry sand, but occasional misclassification of sparse vegetation in wet sand areas.

In comparing the classifiers, SVM provided the smoothest classification outputs, particularly in FS-2, minimizing fragmentation across the landscape. However, RF was the most effective in capturing narrow water channels, a critical feature in the riverine landscape, although it occasionally suffered from scattered sparse vegetation within wet sand areas. GTB, while offering balanced performance, struggled in certain areas, particularly in distinguishing between dry and wet sand, reflecting limitations in handling spectral similarities between these two classes.

For a more comprehensive evaluation of the classifier’s performance, Kappa coefficient and overall accuracy metrics were calculated and are listed in Table 2. These metrics provide quantitative insights into how well each classifier distinguished between the five land cover classes, across the two feature sets. The results demonstrate a clear improvement in classification accuracy and Kappa coefficient when indices are added in FS-2, highlighting the importance of incorporating additional features for remote sensing applications.

Classifier	Feature Set	Kappa coefficient	Overall Accuracy
RF	FS-1	0.70	75.86%
SVM	FS-1	0.81	84.48%
GTB	FS-1	0.73	78.16%
RF	FS-2	0.81	84.48%
SVM	FS-2	0.81	84.48%
GTB	FS-2	0.80	83.91%

Table 2. Kappa coefficient and overall accuracy

RF showed significant improvement with FS-2, where its Kappa coefficient increased from 0.70 to 0.81, and overall accuracy improved from 75.86% to 84.48%. This indicates that the enriched feature set helped reduce confusion between overlapping classes, especially between wet and dry sand, which posed challenges in FS-1. SVM demonstrated high stability, achieving the same Kappa value of 0.81 and an accuracy of 84.48% with both feature sets. This suggests that SVM effectively captures both spectral and spatial variability, providing reliable classifications in complex riverine landscapes.

GTB, while performing well, exhibited slightly lower accuracy compared to RF and SVM. It achieved a Kappa of 0.73 and 78.16% accuracy with FS-1, improving to 0.80 and 83.91% with FS-2. Although the inclusion of indices enhanced its performance, GTB still encountered some difficulty distinguishing between wet sand and sparse vegetation, highlighting its limitations with spectrally similar classes.

The F1-Score heatmap (Figure 3) offers valuable insights highlight the nuanced strengths and weaknesses of each classifier when tasked with mapping complex classes such as wet sand and sparse vegetation within the riverine landscape. For the water class, all classifiers demonstrate marked improvement with FS-2, highlighting the role of indices in enhancing water detection. GTB, in particular, achieves the highest F1-Score for water at 85.33% with FS-2, suggesting that the additional indices helped in better distinguishing water from other reflective surfaces. This improvement underscores how the enriched feature set provides a more refined spectral separation, minimizing confusion with features like wet sand or sparse vegetation that may otherwise exhibit overlapping spectral characteristics. In FS-1, however, the performance of RF and GTB is more moderate, scoring 80.00%, which indicates some misclassification likely due to overlapping spectral properties with wet sand or sparse vegetation near the water bodies.

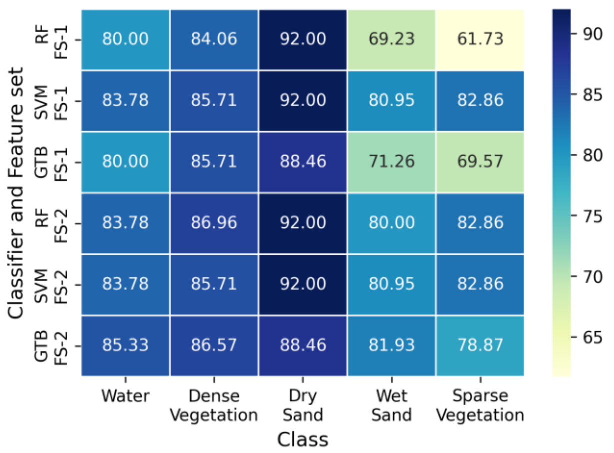

Figure 3. F1-Score heatmap

When classifying dense vegetation, the performance remains stable across both feature sets, with RF achieving the highest F1-Score of 86.96% using FS-2. This consistency across classifiers reflects the distinct spectral signature of dense vegetation, which the classifiers can reliably identify even with minimal input data. However, adding indices in FS-2 further refines the classification, especially for RF, by minimizing misclassifications with sparse vegetation.

The dry sand class exhibits strong performance across all models and feature sets, with RF and SVM consistently achieving F1 scores of 92.00%. This suggests that dry sand possesses clear and distinguishable spectral characteristics, making it easier to classify with high accuracy. The high scores across FS-1 and FS-2 indicate that additional indices provide only marginal improvement for this class, as the classifiers already performed well with the spectral bands alone.

The dry sand class exhibits strong performance across all models and feature sets, with RF and SVM consistently achieving F1 scores of 92.00%. This suggests that dry sand possesses clear and distinguishable spectral characteristics, making it easier to classify with high accuracy. The high scores across FS-1 and FS-2 indicate that additional indices provide only marginal improvement for this class, as the classifiers already performed well with the spectral bands alone.

The classification of wet sand, on the other hand, proves more challenging, especially with FS-1. RF achieves only 69.23% with FS-1, indicating frequent misclassification, possibly as sparse vegetation or dry sand. However, introducing indices in FS-2 leads to significant improvement across all classifiers, with GTB reaching 81.93%. This suggests that the spectral index in FS-2 captures subtle differences in moisture content, improving the identification of wet sand, which often overlaps spectrally with other classes.

Sparse vegetation remains the most difficult class to classify accurately. RF with FS-1 struggles the most, with an F1-Score of 61.73%, suggesting considerable confusion with wet or dry sand. However, the use of FS-2 enhances the ability of the classifier to map sparse vegetation, with RF and SVM achieving 82.86%. However, the results also suggest that some challenges remain, likely due to the spectral similarity between sparse vegetation and certain sand classes. This overlap makes it difficult for the classifiers to consistently separate these categories, indicating that further refinements in feature selection or additional data inputs may be necessary to enhance classification accuracy. Overall, the F1-score analysis indicates that FS-2 consistently improves classification performance by providing extra spectral information, helping to resolve ambiguities in complex land cover classes.

4. Conclusion

This research combined high spatial resolution imagery, albeit limited in spectral resolution, with derived indices to enhance land cover classification accuracy in riverine environments. Utilizing LISS-4 imagery from the IRS-R2 satellite, we developed two distinct feature sets and applied three machine learning classifiers to evaluate their effectiveness in mapping complex land cover types. The inclusion of additional indices in the second feature set (FS-2) significantly improved classification performance, particularly in distinguishing visually similar classes such as wet sand, dry sand, and sparse vegetation, underscoring the critical role of spectral indices in capturing detailed landscape features.

https://doi.org/10.5194/isprs-annals-X-G-2025-813-2025 |

The results demonstrate that the combination of FS-2 and RF provided the most accurate and interpretable output for the riverine environment, especially in delineating narrow channels and sandbars. The inclusion of spectral indices allowed the classifiers to better capture landscape features and spatial variability, which were essential for mapping the dynamic features of the river confluence. This enhancement is further supported by accuracy metrics, including F1-scores, Cohen's Kappa, and overall accuracy, which demonstrated substantial improvements with FS-2, underscoring the value of incorporating additional indices to strengthen classifier performance across challenging classes. However, the persistent confusion between wet sand and sparse vegetation highlights the inherent complexity of the landscape and suggests that further refinement or the addition of texture-based features may be necessary to improve classification accuracy in these areas.

Overall, the results indicate that FS-2 significantly enhances classification outcomes across all classifiers, confirming the importance of integrating spectral indices to improve model accuracy. Both RF and SVM emerge as the most effective classifiers, with RF excelling in mapping narrow water channels and vegetation, while SVM provides smooth, stable classifications across all classes. GTB offers competitive results but lags slightly behind RF and SVM, particularly in accurately separating sand and vegetation classes. Notably, GTB demonstrates considerable improvement with FS-2, especially for complex classes like wet sand. These findings highlight the importance of selecting appropriate feature sets and classifiers to achieve robust and reliable land cover classification in dynamic and heterogeneous landscapes, such as the confluence of the Mahanadi and Shivnath Rivers.

References

Arora, Virat, S. Srinivasa Rao, E. Amminedu, and P. Jagadeeswara Rao. "Feature Selection for Improved Classification Accuracy Targeting Riverine Sand Mapping." Spatial Information Research 29, no. 3 (June 2021): 389–404. https://doi.org/10.1007/s41324-020-00359-1.

Belgiu, Mariana, and Lucian Drăguţ. "Random Forest in Remote Sensing: A Review of Applications and Future Directions." ISPRS Journal of Photogrammetry and Remote Sensing 114 (April 2016): 24–31. https://doi.org/10.1016/j.isprsjprs.2016.01.011.

Boothroyd, Richard J., Richard D. Williams, Trevor B. Hoey, Brian Barrett, and Octria A. Prasojo. "Applications of Google Earth Engine in Fluvial Geomorphology for Detecting River Channel Change." WIREs Water 8, no. 1 (January 2021): e21496. https://doi.org/10.1002/wat2.1496.

Breiman, L., 2001. Random forests. Machine Learning 45(1), 5-32. https://doi.org/10.1023/A:1010950718922.

Cortes, Corinna, and Vladimir Vapnik. "Support-Vector Networks." Machine Learning 20, no. 3 (September 1995): 273–97. https://doi.org/10.1007/BF00994018.

Dmitriev, E.V., T.V. Kondranin, P.G. Melnik, and S.A. Donskoy. "Statistical Texture Analysis of Forest Areas from Very High Spatial Resolution Satellite Images." In Spatial Data Processing for Monitoring of Natural and Anthropogenic Processes 2021, 56–66. Crossref, 2021. https://doi.org/10.25743/SDM.2021.64.23.009.

Foody, Giles M. "Status of Land Cover Classification Accuracy Assessment." Remote Sensing of Environment 80, no. 1 (April 2002): 185–201. https://doi.org/10.1016/S0034-4257(01)00295-4.

Gitelson, Anatoly A., Yoram J. Kaufman, and Mark N. Merzlyak. "Use of a Green Channel in Remote Sensing of Global Vegetation from EOS-MODIS." Remote Sensing of Environment 58, no. 3 (December 1996): 289–98. https://doi.org/10.1016/S0034-4257(96)00072-7.

Huete, A.R. "A Soil-Adjusted Vegetation Index (SAVI)." Remote Sensing of Environment 25, no. 3 (August 1988): 295–309. https://doi.org/10.1016/0034-4257(88)90106-X.

McFEETERS, S. K. "The Use of the Normalized Difference Water Index (NDWI) in the Delineation of Open Water Features." International Journal of Remote Sensing 17, no. 7 (May 1996): 1425–32. https://doi.org/10.1080/01431169608948714.

Natekin, Alexey, and Alois Knoll. "Gradient Boosting Machines, a Tutorial." Frontiers in Neurorobotics 7 (2013). https://doi.org/10.3389/fnbot.2013.00021.

Ouchra, Hafsa, Abdessamad Belangour, and Allae Erraissi. "Machine Learning Algorithms for Satellite Image Classification Using Google Earth Engine and Landsat Satellite Data: Morocco Case Study." IEEE Access 11 (2023): 71127–42. https://doi.org/10.1109/ACCESS.2023.3293828.

Pal, M., and P. M. Mather. "Support Vector Machines for Classification in Remote Sensing." International Journal of Remote Sensing 26, no. 5 (March 2005): 1007–11. https://doi.org/10.1080/01431160512331314083.

Penuelas, J., J. Pinol, R. Ogaya, and I. Filella. "Estimation of Plant Water Concentration by the Reflectance Water Index WI (R900/R970)." International Journal of Remote Sensing 18, no. 13 (September 1997): 2869–75. https://doi.org/10.1080/014311697217396.

Pinty, B., and M. M. Verstraete. "GEMI: A Non-Linear Index to Monitor Global Vegetation from Satellites." Vegetatio 101, no. 1 (July 1992): 15–20. https://doi.org/10.1007/BF00031911.

Rahman, Ashikur, Hasan Muhammad Abdullah, Md Tousif Tanzir, Md Jakir Hossain, Bhoktear M. Khan, Md Giashuddin Miah, and Imranul Islam. "Performance of Different Machine Learning Algorithms on Satellite Image Classification in Rural and Urban Setup." Remote Sensing Applications: Society and Environment 20 (November 2020): 100410. https://doi.org/10.1016/j.rsase.2020.100410.

Rajesh, S., T. Gladima Nisia, S. Arivazhagan, and R. Abisekaraj. "Land Cover/Land Use Mapping of LISS IV Imagery Using Object-Based Convolutional Neural Network with Deep Features." Journal of the Indian Society of Remote Sensing 48, no. 1 (January 2020): 145–54. https://doi.org/10.1007/s12524-019-01064-9.

Rodriguez-Galiano, V.F., B. Ghimire, J. Rogan, M. Chica-Olmo, and J.P. Rigol-Sanchez. "An Assessment of the Effectiveness of a Random Forest Classifier for Land-Cover Classification." ISPRS Journal of Photogrammetry and Remote Sensing 67 (January 2012): 93–104. https://doi.org/10.1016/j.isprsjprs.2011.11.002.

Rondeaux, Geneviève, Michael Steven, and Frédéric Baret. “Optimization of Soil-Adjusted Vegetation Indices.” Remote Sensing of Environment 55, no. 2 (February 1996): 95–107. https://doi.org/10.1016/0034-4257(95)00186-7.

Rouse, W, and R H Haas. “MONITORING VEGETATION SYSTEMS IN THE GREAT PLAINS WITH ERTS,” n.d.

Swati Vishnoi, and Meenakshi Pareek. “Contextual Based Hybrid Classification with FCM to Handle Mixed Pixels and Edge Preservation.” International Journal of Information Technology 16, no. 6 (August 2024): 3537–47. https://doi.org/10.1007/s41870-024-01959-y.

Tadese, Mahtsente, Lalit Kumar, Richard Koech, and Benjamin K. Kogo. “Mapping of Land-Use/Land-Cover Changes and Its Dynamics in Awash River Basin Using Remote Sensing and GIS.” Remote Sensing Applications: Society and Environment 19 (August 2020): 100352. https://doi.org/10.1016/j.rsase.2020.100352.

Talukdar, Swapan, Pankaj Singha, Susanta Mahato, Shahfahad, Swades Pal, Yuei-An Liou, and Atiqur Rahman. “Land-Use Land-Cover Classification by Machine Learning Classifiers for Satellite Observations—A Review.” Remote Sensing 12, no. 7 (April 2, 2020): 1135. https://doi.org/10.3390/rs12071135.

Tobón-Marín, Alejandro, and Julio Cañón Barriga. “Analysis of Changes in Rivers Planforms Using Google Earth Engine.” International Journal of Remote Sensing 41, no. 22 (November 16, 2020): 8654–81. https://doi.org/10.1080/01431161.2020.1792575.

Verma, Amit Kumar, P. K. Garg, K. S. Hari Prasad, and V. K. Dadhwal. “CLASSIFICATION OF LISS IV IMAGERY USING DECISION TREE METHODS.” ISPRS - International Archives of the Photogrammetry, Remote Sensing and Spatial Information Sciences XLI-B8 (June 24, 2016): 1061–66. https://doi.org/10.5194/isprsarchives-XLI-B8-1061-2016.

Zhang, Kaili, Yonggang Chen, Wentao Wang, Yudi Wu, Bo Wang, and Yanting Yan. “A Method for Remote Sensing Image Classification by Combining Pixel Neighbourhood Similarity and Optimal Feature Combination.” Geocarto International 38, no. 1 (December 31, 2023): 2158948. https://doi.org/10.1080/10106049.2022.2158948.